

## Vibronic Transitions of $\text{Sm}^{2+}$ and $\text{Eu}^{2+}$ in $\text{SrF}_2$ and Their Zeeman Effect

E. COHEN AND H. J. GUGGENHEIM

*Bell Telephone Laboratories, Murray Hill, New Jersey 07974*

(Received 13 June 1968)

The vibronic emission spectra of  $\text{Sm}^{2+}$  and  $\text{Eu}^{2+}$  in  $\text{SrF}_2$  have been studied at low temperatures. The Zeeman effect of the transitions  ${}^5D_0(\Gamma_1^+) \rightarrow {}^7F_1(\Gamma_4^+)$  and  ${}^7F_2(\Gamma_6^+)$  of  $\text{Sm}^{2+}$  was observed with fields up to 70 kOe applied along the [100] axis. The vibronic spectra of  $\text{Sm}^{2+}$  associated with electronic transitions within the  $4f^6$  configuration cut off sharply at phonon energy of  $310 \text{ cm}^{-1}$ . Several sharp peaks are observed within this range. The vibronic spectrum accompanying the transition  $4f^6 5d(\Gamma_8^+) \rightarrow 4f^7 {}^8S_{7/2}(\Gamma_6^- + \Gamma_7^- + \Gamma_8^-)$  of  $\text{Eu}^{2+}$  spreads up to eight-phonon excitations, with sharp peaks appearing in the region of single-phonon excitations. The vibronic transitions of both ions are shown to have electric dipole character. Then a comparison between phonon energies derived from the vibronic spectra of  $\text{Sm}^{2+}$  and  $\text{Eu}^{2+}$  determines the parity of the vibrations at the rare-earth-ion site. By using selection rules for vibronic transitions associated with the  $\Gamma_i^+ \rightarrow \Gamma_i^+$  ( $i=1, \dots, 5$ ) transitions of  $\text{Sm}^{2+}$ , the number of possible irreducible representations to which the vibration belongs is reduced. Further reduction of this number is obtained by examining the polarization of the vibronic Zeeman components. It is found that only one of the potential components set up by the phonon at the rare-earth site has the main contribution to the vibronic intensity. In most cases this is the component which transforms like  $\Gamma_4^-$ , presumably because of the electric field, but components transforming like  $\Gamma_1^-$  and  $\Gamma_3^-$  are also observed.

### I. INTRODUCTION

**D**IVALENT rare-earth (RE) ions in alkaline-earth fluorides occupy predominantly the cubic sites of the metal which they replace. Their optical spectrum consists of electronic transitions within the  $4f^n$  configuration, between the  $4f^{n-1}5d$  and  $4f^n$  configurations and a wealth of vibronics accompanying these transitions. The energies of the phonons involved were deduced from the vibronic transitions of several divalent rare-earth ions.<sup>1-7</sup> The effect of selection rules governing the vibronic transitions was recognized by Weakliem and Kiss<sup>6</sup> in the spectrum of  $\text{Ho}^{2+}$ . Several attempts were made<sup>2,4,5,8</sup> to classify the phonons involved by assuming that the transitions had electric dipole character. Since no information was available on the phonon frequency distribution function (except for the energy of the  $\mathbf{k}=0$  modes) the assignment of phonon symmetries and the character of the vibronic transitions remained speculative only. In the present study, the character of the vibronic transitions is examined by the use of their Zeeman effect. Also, making use of symmetry selection rules,<sup>9</sup> information is obtained on the types of phonons which contribute to the vibronic spectrum of divalent rare-earth ions. In general, the vibronic spectrum appears to consist of broad bands

on which relatively sharp lines are superimposed. The transitions within the  $4f^n$  configuration involving excitation of single phonons are several orders of magnitude stronger than those which involve the creation of two or more phonons. On the other hand, for transitions between the  $4f^{n-1}5d$  and  $4f^n$  configurations, vibronics which involve the simultaneous creation of several phonons appear with comparable intensities. It is found that all observed vibronic transitions have electric dipole character. The phonons contributing to such transitions have  $\mathbf{k}$  along directions or at points of high symmetry in the Brillouin zone.

The system of a divalent rare-earth ion in  $\text{MeF}_2$  is an attractive one because of the high site symmetry ( $O_h$ ) of the rare-earth ion and the small number of phonon branches (9).  $\text{Sm}^{2+}$  and  $\text{Eu}^{2+}$  in  $\text{SrF}_2$  appear to be most favorable for several reasons. The ionic radius of  $\text{Sr}^{2+}$  (1.13 Å) is closer to that of  $\text{Sm}^{2+}$  (1.11 Å) and  $\text{Eu}^{2+}$  (1.12 Å) than those of  $\text{Ca}^{2+}$  and  $\text{Ba}^{2+}$ . Although the rare-earth ion's mass is 1.7 times that of Sr, it is expected that the vicinity of the rare-earth ion will be less distorted when its ionic radius is close to that of the ion it substitutes. In  $\text{SrF}_2$  (and  $\text{BaF}_2$ ), the  $4f^6 {}^5D_0$  level of  $\text{Sm}^{2+}$  lies below the  $4f^6 5d$  levels<sup>1</sup> so that it is possible to study the fluorescence vibronic spectrum within the  $4f^6$  configuration. This is not the case for  $\text{Sm}^{2+}:\text{CaF}_2$ , where all the emission at low temperatures originates at a  $4f^6 5d(\Gamma_1^-)$  level. In the case of  $\text{Eu}^{2+}$  in all three  $\text{MeF}_2$ , the transitions are between the lowest  $4f^6 5d$  state and the  $4f^7 {}^8S_7$  ground state. Comparing the fluorescence spectra of both  $\text{Sm}^{2+}$  and  $\text{Eu}^{2+}$  in  $\text{BaF}_2$  and  $\text{SrF}_2$  it is noted that the intensities in the latter are much higher, thus enabling us to uncover fine details of the vibronic spectrum. Since the  $\text{Sm}^{2+}$  transitions involve electronic states having the same parity and those of  $\text{Eu}^{2+}$  states of opposite parity, a comparison be-

<sup>1</sup> D. L. Wood and W. Kaiser, Phys. Rev. **126**, 2079 (1962), ( $\text{Sm}^{2+}$ ).

<sup>2</sup> I. Richman, Phys. Rev. **133**, A1364 (1964), ( $\text{Sm}^{2+}$ ).

<sup>3</sup> A. A. Kaplyanskii and A. K. Przhhevskii, Opt. i Spektroskopiya **19**, 597 (1965) [English transl.: Opt. Spectry. (USSR) **19**, 331 (1965)], ( $\text{Eu}^{2+}$ ).

<sup>4</sup> M. V. Hobden, Phys. Letters **15**, 10 (1965), ( $\text{Eu}^{2+}$ ).

<sup>5</sup> Z. J. Kiss, Phys. Rev. **137**, A1749 (1965), ( $\text{Dy}^{2+}$ ).

<sup>6</sup> H. A. Weakliem and Z. J. Kiss, Phys. Rev. **157**, 277 (1967), ( $\text{Ho}^{2+}$ ).

<sup>7</sup> Z. J. Kiss, Phys. Rev. **127**, 718 (1962), ( $\text{Tm}^{2+}$ ).

<sup>8</sup> J. D. Axe and P. P. Sorokin, Phys. Rev. **130**, 945 (1963).

<sup>9</sup> R. Loudon, Proc. Phys. Soc. (London) **84**, 379 (1964).

tween their vibronic spectra provides information on the parity of the phonons involved. This, together with the Zeeman effect, is essential in determining the operating selection rules.

## II. EXPERIMENTAL PROCEDURE

The crystals employed in this study were grown by a horizontal zone refining method. The Sm-doped crystal was subsequently treated by electrolysis to convert  $\text{Sm}^{3+}$  to  $\text{Sm}^{2+}$ .<sup>10</sup> The  $\text{Sm}:\text{SrF}_2$  sample contained approximately 0.1%  $\text{Sm}^{2+}$  while the  $\text{Eu}:\text{SrF}_2$  sample contained less than 0.01%  $\text{Eu}^{2+}$ . Fluorescence was obtained by irradiating the crystals with the properly filtered output of a 1000-W Hg-Xe lamp. For wavelength determination of the emission lines, photographic plates were taken on a 2-m Bausch and Lomb spectrograph. This spectrograph employed a  $4\times 8$ -in. grating with 300 l/mm and was used in the fifth to eighth orders. Intensities were measured with a 1-m Jarrel-Ash spectrometer employing a  $4\times 4$ -in. grating with 1200 l/mm in second and third orders, and equipped with an EMI 9558B photomultiplier tube. The intensities were corrected for variations in the photomultiplier sensitivity with wavelength. The emission spectrum of  $\text{Eu}^{2+}$  was obtained at 4.2°K and that of  $\text{Sm}^{2+}$  at 1.6, 4.2, 20.4, and 74°K. The Zeeman effect of the  $\text{Sm}^{2+}$  transitions was taken by applying an external magnetic field along the [100] direction. Fields up to 23 kOe were obtained by using an electromagnet. In this setup the crystal was immersed in the coolant. Fields up to 70 kOe were obtained using a superconducting magnet, in which case the crystal was cooled by exchange He gas and the temperature was estimated to be 5°K.

## III. EXPERIMENTAL RESULTS

### A. Electronic Transitions of $\text{Sm}^{2+}$

The most intense fluorescence of  $\text{Sm}^{2+}$  in  $\text{SrF}_2$  at low temperatures originates at the  ${}^5D_0(\Gamma_1^+)$  level and terminates on the various Stark components of the  ${}^7F_J$  ( $J=0, 1, \dots, 6$ ) multiplet. Since the site symmetry is  $O_h$ , the following selection rules hold: The transition  $\Gamma_1^+ \rightarrow \Gamma_4^+(T_{1g})$  is magnetic dipole (MD) allowed and the transitions  $\Gamma_1^+ \rightarrow \Gamma_3^+(E_g)$  and  $\Gamma_5^+(T_{2g})$  are electric quadrupole allowed.<sup>11</sup> As described by Wood and Kaiser,<sup>1</sup> the  $\Gamma_1^+ \rightarrow \Gamma_4^+$  are the strongest of all electronic transitions, in particular the transition  ${}^5D_0(\Gamma_1^+) \rightarrow {}^7F_1(\Gamma_4^+)$ , indicating that the free-ion  $J$ -selection rule is still operative. Most of the other electronic transitions, though much weaker, are still observed at 4.2 and 20.4°K. At 77°K they are not observed and the intensity of the  ${}^5D_0 \rightarrow {}^7F_1$  transition is three times smaller

<sup>10</sup> H. J. Guggenheim and J. V. Kane, Appl. Phys. Letters 4, 172 (1964).

<sup>11</sup> The notation employed here is that of G. E. Koster *et al.*, *Properties of the Thirty-Two Point Groups* (The M.I.T. Press, Cambridge, Mass., 1963).

TABLE I. Vibronic transitions of  $\text{Sm}^{2+}$  in  $\text{SrF}_2$  (at 4.2°K) associated with the transition  ${}^5D_0 \rightarrow {}^7F_0(\Gamma_1^+)$ .

$\bar{\nu}$ (cm <sup>-1</sup> )	$\Delta\bar{\nu}$	$I_{ab}$	$I_{tot}$	Remarks
14 612.6	0	$4.5\times 10^{-4}$	$4\times 10^{-4}$	
14 609.6		$4.4\times 10^{-4}$	$4.4\times 10^{-4}$	
14 605.4		$4.4\times 10^{-5}$	$4.4\times 10^{-5}$	
14 526	87	$1.5\times 10^{-3}$	$1.9\times 10^{-3}$	center of band
14 517	96			edge of band
14 481.9	130.7	$4.4\times 10^{-5}$	$6\times 10^{-4}$	
14 469	144			broad; 20.4°K
14 456	157	$1.3\times 10^{-4}$	$6\times 10^{-4}$	broad
14 447.3	165.3			weak
14 429.2	183.4	$4.6\times 10^{-5}$	$8\times 10^{-4}$	
14 418.6	194.0	$3.7\times 10^{-4}$	$2.3\times 10^{-3}$	
14 410.5	202.1	$1.8\times 10^{-4}$	$3.2\times 10^{-3}$	
14 389	223	$7\times 10^{-4}$	$1.2\times 10^{-2}$	broad
14 358.4	254.2			
14 328.4	284.0			
14 318.7	293.9	$7.5\times 10^{-3}$	$2.5\times 10^{-3}$	
14 312.4	300.2			weak
14 302	310			edge of band
14 268	343	$2.2\times 10^{-3}$	$2.2\times 10^{-3}$	broad

than that at 4.2°K. All the electronic transitions studied here, namely,  ${}^5D_0 \rightarrow {}^7F_0$ ,  ${}^7F_1$ ,  ${}^7F_2(\Gamma_5^+)$ ,  ${}^7F_2(\Gamma_3^+)$ , consist of several closely spaced lines, where only a single line is expected (see Table I). In the case of the  ${}^5D_0 \rightarrow {}^7F_1$  transition, the MD-allowed transition is 100 times stronger than the close-lying satellites. However, for other observed electronic transitions, all close-lying lines have comparable intensities. It is therefore important to determine which of the observed lines is the no-phonon line. This is best done by comparing the energies of the phonons giving rise to the sharpest vibronic transitions associated with a given electronic transition, with those associated with the  ${}^5D_0 \rightarrow {}^7F_1$  transition. It is found that the position of the no-phonon line, obtained in this manner, coincides with the position of the strongest line of each of these groups. Also, in the case of the  ${}^5D_0(\Gamma_1^+) \rightarrow {}^7F_2(\Gamma_5^+)$  transition, the no-phonon line so determined is the only one out of the three closely spaced lines which shows a Zeeman effect. We therefore conclude that the extra lines are due to  $\text{Sm}^{2+}$  ions located at sites of symmetry lower than cubic. Apparently, the symmetry is low enough to split the triply degenerate  $\Gamma_4^+$  and  $\Gamma_5^+$  states so that no first-order Zeeman effect is observed for the satellites.

### B. Vibronic Transitions of $\text{Sm}^{2+}$

The fluorescence vibronic transitions associated with the transitions  ${}^5D_0(\Gamma_1^+) \rightarrow {}^7F_0(\Gamma_1^+)$ ,  ${}^7F_1(\Gamma_4^+)$ ,  ${}^7F_2(\Gamma_5^+)$ , and  ${}^7F_2(\Gamma_3^+)$  of  $\text{Sm}^{2+}$  are shown in Fig. 1. These are the only parent transitions for which there is no overlap of the associated vibronics and, therefore, it is they that are most suitable for this study. Generally, the vibronic spectrum consists of a broad band, starting at phonon energy of  $\sim 60$  cm<sup>-1</sup> and cutting off sharply at 310 cm<sup>-1</sup>. An additional weak band appears with

TABLE II. Vibronic transitions of  $\text{Sm}^{2+}$  in  $\text{SrF}_2$  (at  $4.2^\circ\text{K}$ ) associated with the transition  ${}^5D_0 \rightarrow {}^7F_1(\Gamma_4^+)$  and Zeeman effect with  $H \parallel [100]$ .

$\tilde{\nu}$ ( $\text{cm}^{-1}$ )	$\Delta\tilde{\nu}$	$I_{ab}$	$I_{tot}$	$\sigma$	$Z_T$	$\pi$	$\sigma^-$	$Z_L$	$\sigma^+$
14 349.1	0	1	1	0		$\pm 1$			
14 263	86	$2.2 \times 10^{-3}$	$2.2 \times 10^{-3}$						center of band
14 171	178	$5 \times 10^{-5}$	$4 \times 10^{-4}$	$\pm 1$		0		$\pm 1$	
14 167	182	$5 \times 10^{-5}$	$4 \times 10^{-4}$						
14 146.6	202.5	$5 \times 10^{-5}$	$10^{-3}$	$\pm 1, 0$		$\pm 1$	$+1, 0$		$-1, 0$
14 125.5	223.6	$2.5 \times 10^{-4}$	$1.7 \times 10^{-3}$	$\pm 1, 0$		$\pm 1$	$+1, 0$		$-1, 0$
14 099.4	249.7	$5 \times 10^{-5}$	$1.5 \times 10^{-3}$						
14 094.9	254.2	$5 \times 10^{-5}$	$1.5 \times 10^{-3}$	$\pm 1, 0$		$\pm 1$	$+1, 0$		$-1, 0$
14 088.7	260.4	$1.6 \times 10^{-4}$	$1.5 \times 10^{-3}$						
14 055.1	294.0	$1.1 \times 10^{-3}$	$2.5 \times 10^{-3}$	$\pm 1, 0$		$\pm 1$	$+1, 0$		$-1, 0$
14 049	300								
14 038	311								edge of band
14 009	340	$2.5 \times 10^{-4}$	$2.5 \times 10^{-4}$						

peak intensity at a phonon energy of  $\sim 340 \text{ cm}^{-1}$ . The sharp cutoff of the vibronic spectrum at approximately the end of the single-phonon excitation is characteristic of transitions within the  $4f^n$  configuration as observed for  $\text{RECl}_3$ .<sup>12</sup> Several peaks appear on the broad emission band, with width varying between 2–10  $\text{cm}^{-1}$  and with intensity which depends on the final electronic transition. The data obtained for these sharp lines are compiled in Tables I–IV. From the frequency of the observed vibronic ( $\tilde{\nu}$ ), the energy of the phonon is determined ( $\Delta\tilde{\nu}$ ). The intensity of a given vibronic transition is given relative to the intensity of the MD-allowed electronic transition  ${}^5D_0 \rightarrow {}^7F_1$ , which is arbitrarily chosen to be unity. There are two figures quoted for the intensity:  $I_{ab}$ , the intensity above the background emission, and  $I_{tot}$ , the total intensity.  $I_{ab}$  is obviously dependent on where one chooses the background level to be. It is, therefore, not as accurate a quantity as is the total intensity of the line  $I_{tot}$ . However,  $I_{ab}$  still gives an idea on the strength of a particular vibronic line, which cannot be judged from its total intensity.

Since all transitions originate from a  $\Gamma_1^+$  state which has no Zeeman effect, their Zeeman effect depends on the terminal electronic state. Thus, Zeeman effect is obtained for those transitions associated with the  $\Gamma_4^+$  and  $\Gamma_5^+$  terminal states. The polarization of the observed Zeeman components is given in the last four columns of Tables II and III. The external magnetic field is applied along the  $[100]$  direction and the polarization is that of the electric vector of the light with respect to the applied magnetic field. The symbols 0, +1, and -1 for  $\Gamma_4^+$  and 2, +1, and -1 for  $\Gamma_5^+$  are the magnetic quantum numbers of the final vibronic states of a transition observed in the particular polarization. In the transverse Zeeman-effect configuration ( $Z_T$ ), the crystal is viewed along the  $[001]$  direction which is perpendicular to the magnetic field. In the longitudinal configuration ( $Z_L$ ), the crystal is viewed along the direction of the field.

The splitting factors of the electronic states are found to be identical with those reported by Wood and Kaiser.<sup>1</sup> It is difficult to obtain very accurate splitting

TABLE III. Vibronic transitions of  $\text{Sm}^{2+}$  in  $\text{SrF}_2$  (at  $4.2^\circ\text{K}$ ) associated with the transition  ${}^5D_0 \rightarrow {}^7F_2(\Gamma_5^+)$  and Zeeman effect with  $H \parallel [100]$ .

$\tilde{\nu}$ ( $\text{cm}^{-1}$ )	$\Delta\tilde{\nu}$	$I_{ab}$	$I_{tot}$	$\sigma$	$Z_T$	$\pi$	$\sigma^-$	$Z_L$	$\sigma^+$
13 961.5	0	$1.5 \times 10^{-4}$	$1.5 \times 10^{-4}$	2		$\pm 1$			
13 958.8									
13 957.1									
13 863.3	97.4	$3.2 \times 10^{-4}$	$7 \times 10^{-4}$	$\pm 1$		2	$+1, -1^a$		$-1, +1^a$
13 793.1	167.6	$7 \times 10^{-4}$	$3 \times 10^{-3}$	$\pm 1$		2	$+1, -1^a$		$-1, +1^a$
13 765.6	195.1	$4 \times 10^{-5}$	$3.2 \times 10^{-3}$	$\pm 1$		2	$+1, -1^a$		$-1, +1^a$
13 740	222	$1.9 \times 10^{-3}$	$3.8 \times 10^{-3}$						
13 711.5	249.2	$4 \times 10^{-5}$	$1.6 \times 10^{-3}$	$\pm 1, 2$		$\pm 1$	$+1, 2$		$-1, 2$
13 706.2	254.5	$4 \times 10^{-5}$	$1.6 \times 10^{-3}$	$\pm 1, 2$		$\pm 1$	$+1, 2$		$-1, 2$
13 700.5	260.2	$4 \times 10^{-5}$	$1.6 \times 10^{-3}$	$\pm 1, 2$		$\pm 1$	$+1, 2$		$-1, 2$
13 667.1	293.6	$4 \times 10^{-4}$	$2 \times 10^{-3}$	$\pm 1, 2$		$\pm 1$	$+1, 2$		$-1, 2$
13 661.3	299.4								
13 651	310								edge of band
13 620	341	$1.7 \times 10^{-4}$	$1.7 \times 10^{-4}$						

<sup>a</sup> Appears weaker in this polarization.<sup>12</sup> E. Cohen and H. W. Moos, Phys. Rev. **161**, 258 (1967).

factors for the vibronic lines, because their width allows observation of the Zeeman effect at high fields only. However, they appear to follow closely the splitting factor of their parent transitions.

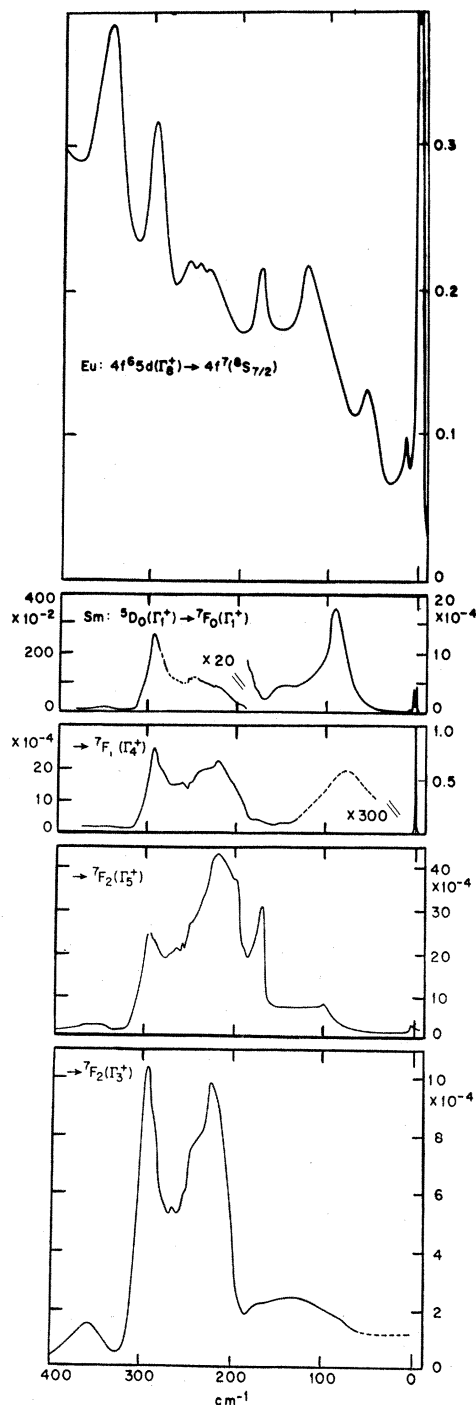


FIG. 1. Vibronic spectra of  $\text{Sm}^{2+}$  in  $\text{SrF}_2$  associated with the electronic transitions  ${}^5D_0(\Gamma_1^+) \rightarrow {}^7F_0(\Gamma_1^+)$ ,  ${}^7F_1(\Gamma_4^+)$ , and  ${}^7F_2(\Gamma_5^+$  and  $\Gamma_3^+)$ . A portion of the vibronic spectrum of  $\text{Eu}^{2+}$  in  $\text{SrF}_2$  corresponding to single-phonon excitation is shown on top. The abscissa gives the phonon energy and the ordinate relative emission intensity. (Observation done at  $4.2^\circ\text{K}$ .)

TABLE IV. Vibronic transitions of  $\text{Sm}^{2+}$  in  $\text{SrF}_2$  (at  $4.2^\circ\text{K}$ ) associated with the transition  ${}^5D_0 \rightarrow {}^7F_2(\Gamma_3^+)$ .

$\tilde{\nu}$ ( $\text{cm}^{-1}$ )	$\Delta\tilde{\nu}$	$I_{\text{ab}}$	$I_{\text{tot}}$
13 588.0			
13 577.8	0		$<10^{-5}$
13 567.7			
13 558.7			
13 354	225	$8 \times 10^{-4}$	$1.1 \times 10^{-3}$
13 342	237	$6 \times 10^{-4}$	$8 \times 10^{-4}$
13 323	256		$6 \times 10^{-4}$
13 318	261		$6 \times 10^{-4}$
13 295	284	$3 \times 10^{-4}$	$1.0 \times 10^{-3}$
13 285	294	$4 \times 10^{-4}$	$1.1 \times 10^{-3}$

In raising the crystal temperature from 1.6 to  $\sim 75^\circ\text{K}$ , a slight reduction in the intensity of the vibronic transitions is observed but no change in their width or energy. However, strong emission from the lowest  $4f^5 5d$  level ( $\Gamma_1^-$ ) to  $4f^6 {}^7F_1$  takes place. The vibronic sideband of this transition consists mainly of a broad band extending up to several hundred wavenumbers from the no-phonon line. Only few peaks could be identified and are reported in Table V(a). At temperatures above  $\sim 80^\circ\text{K}$ , the emission from the  $4f^6 {}^5D_0$  level is weak compared to that from the  $4f^6 5d(\Gamma_1^-)$  level (which lies  $190 \text{ cm}^{-1}$  higher), and the whole vibronic spectrum has a broad band appearance.

### C. Electronic and Vibronic Spectrum $\text{Eu}^{2+}$

The emission spectrum of  $\text{Eu}^{2+}$  under uv excitation consists of the electronic transition  $4f^6 5d(\Gamma_8^+) \rightarrow 4f^7 {}^8S_{7/2}(\Gamma_6^- + \Gamma_7^- + \Gamma_8^-)$  and its vibronic sideband.<sup>3,4,13</sup> Figure 2 shows this spectrum, taken at  $4.2^\circ\text{K}$ . The energies of the phonons involved in the vibronic transitions and their intensity relative to the no-phonon line are given in Table V. While the vibronic spectrum associated with the  $4f^6$  transitions of  $\text{Sm}^{2+}$  cuts off sharply at the end of single-phonon excitation, that of  $\text{Eu}^{2+}$  extends to about eight-phonon excitation. Also, the peak intensity of the  $4f^6$  vibronic spectrum of  $\text{Sm}^{2+}$  is three to five orders of magnitude smaller than the electronic transition. In contrast, the vibronics associated with the  $4f^6 5d-4f^7$  transition of  $\text{Eu}^{2+}$  have intensity comparable to that of the electronic line. The vibronic transitions involving single-phonon excitation show prominent peaks superimposed on a broad band. In the energy region corresponding to the simultaneous excitation of two and three phonons, weaker and broader peaks are observed. The broad background observed here is typical of  $4f^{n-1} 5d-4f^n$  vibronic transitions and was previously observed for many other systems.<sup>14,15</sup>

<sup>13</sup> B. P. Zakharchenya, I. B. Rusanov, and A. Ya. Ryskin, Opt. i Spektroskopiya **13**, 999 (1965) [English transl.: Opt. Spectry. (USSR) **13**, 563 (1965)].

<sup>14</sup> M. Wagner and W. E. Bron, Phys. Rev. **139**, A273 (1965); **145**, 689 (1966).

<sup>15</sup> T. S. Piper, J. P. Brown, and D. S. McClure, J. Chem. Phys. **46**, 1353 (1967).

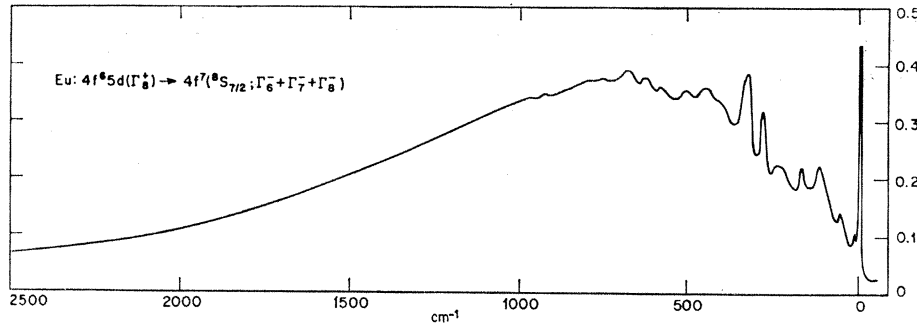


FIG. 2. Vibronic spectrum of  $\text{Eu}^{2+}$  in  $\text{SrF}_2$  at  $4.2^\circ\text{K}$ . Abscissa gives the phonon energy and ordinate gives the vibronic intensity relative to that of the no-phonon line.

The Zeeman effect of the electronic transition (in  $\text{CaF}_2$ ) was investigated by Zakharchenya *et al.*<sup>13</sup> From their results it is seen that the separation between the Zeeman components (at a field of 40 kOe) of both ground and excited states is smaller than the width of the phonons lines. Consistent with this, no Zeeman effect was seen for the  $\text{Eu}^{2+}$  vibronic transitions.

#### IV. ANALYSIS

##### A. Origin of Vibronic Transitions

The observed vibronic transitions arise from the coupling of the RE ion to the phonons by the dynamic part of the crystalline field. In first approximation, the vibronic interaction is linear in the phonon normal coordinates:

$$V_{ev} = \sum_{\mathbf{k}\Gamma^s} f_{\mathbf{k}\Gamma^s} Q_{\mathbf{k}\Gamma^s},$$

where  $f_{\mathbf{k}\Gamma^s}$  operates on the RE electronic coordinates and  $Q_{\mathbf{k}\Gamma^s}$  on the phonon coordinates only. Because the vibronic transition occurs at the RE ion site,  $V_{ev}$  is invariant under the site symmetry group ( $O_h$ ) only. Therefore, the normal coordinates of all phonons in the star of  $\mathbf{k}$  are used to form linear combinations  $Q_{\mathbf{k}\Gamma^s}$  which belong to the  $s$  row of the  $\Gamma$  irreducible representation of the RE site symmetry group.

In the case of  $\text{Sm}^{2+}$  in  $\text{SrF}_2$ , we know that all observed vibronics are electric dipole transitions, since the  $\sigma$ -

polarized lines in the transverse Zeeman effect coincide with the longitudinal Zeeman spectrum. Therefore, the final vibronic state, in which a single phonon is excited, is a predominantly  $4f^6$  state with a slight admixture of  $4f^6 5d$  states (or other odd-parity states which belong to higher configurations). The electric dipole matrix element for a transition between the  ${}^5D_0(\Gamma_1^+)$  state, with all phonons in the ground state, and a  ${}^7F_J(\Gamma_r^+)$  state, with a single phonon excited, is given by

$$\begin{aligned} \langle {}^7F_J(\Gamma_r^+), 1 | P^{[1]} | {}^5D_0(\Gamma_1^+), 0 \rangle &= \sum_{\Gamma_p^-} \left( \frac{\hbar}{2\omega_{\mathbf{k}\Gamma}} \right)^{1/2} \\ &\times \left[ \frac{\langle {}^7F_J(\Gamma_r^+) | f_{\mathbf{k}\Gamma^s} | \Gamma_p^- \rangle \langle \Gamma_p^- | P^{[1]} | {}^5D_0(\Gamma_1^+) \rangle}{E({}^7F_J(\Gamma_r^+)) + \hbar\omega_{\mathbf{k}\Gamma} - E(\Gamma_p^-)} \right. \\ &\left. + \frac{\langle {}^7F_J(\Gamma_r^+) | P^{[1]} | \Gamma_p^- \rangle \langle \Gamma_p^- | f_{\mathbf{k}\Gamma^s} | {}^5D_0(\Gamma_1^+) \rangle}{E({}^5D_0(\Gamma_1^+)) - (\hbar\omega_{\mathbf{k}\Gamma} + E(\Gamma_p^-))} \right]. \end{aligned}$$

The sum extends over all  $4f^6 5d$  states [whose energies are  $E(\Gamma_p^-)$ ] which give nonvanishing matrix elements.

In the case of  $\text{Eu}^{2+}$ , the electronic transition  $4f^6 5d(\Gamma_8^+) \rightarrow 4f^7 {}^8S_{7/2}(\Gamma_6^- + \Gamma_7^- + \Gamma_8^-)$  is electric dipole allowed. The intensity of the vibronics is comparable to that of the electronic transition which they accompany, indicating that they too have electric dipole character. The electric dipole matrix element for a transition between these states in which one phonon is excited is given by

$$\begin{aligned} \langle 4f^7 {}^8S_{7/2}, 1 | P^{[1]} | 4f^6 5d(\Gamma_8^+), 0 \rangle &= \sum_{\Gamma_p^-} \left( \frac{\hbar}{2\omega_{\mathbf{k}\Gamma}} \right)^{1/2} \frac{\langle 4f^7 {}^8S_{7/2} | f_{\mathbf{k}\Gamma^s} | 4f^7 \Gamma_p^- \rangle \langle 4f^7 \Gamma_p^- | P^{[1]} | 4f^6 5d(\Gamma_8^+) \rangle}{(E(4f^7 {}^8S_{7/2}) + \hbar\omega_{\mathbf{k}\Gamma}) - E(4f^7 \Gamma_p^-)} \\ &+ \sum_{\Gamma_q^+} \left( \frac{\hbar}{2\omega_{\mathbf{k}\Gamma}} \right)^{1/2} \frac{\langle 4f^7 {}^8S_{7/2} | P^{[1]} | 4f^6 5d(\Gamma_q^+) \rangle \langle 4f^6 5d(\Gamma_q^+) | f_{\mathbf{k}\Gamma^s} | 4f^6 5d(\Gamma_8^+) \rangle}{E(4f^6 5d(\Gamma_8^+)) - (\hbar\omega_{\mathbf{k}\Gamma} + E(\Gamma_q^+))}. \end{aligned}$$

The contribution of the first sum is negligible in comparison to the second sum because of the following reasons: (a) The first excited states of the  $4f^7$  configuration lie some  $30\,000\text{ cm}^{-1}$  above the ground state,  ${}^8S_{7/2}$ . On the other hand, there are  $4f^6 5d$  states separated by few hundred  $\text{cm}^{-1}$  from the  $4f^6 5d(\Gamma_8^+)$  state.<sup>16</sup> Thus,

<sup>16</sup> A. A. Kaplyanskii and P. P. Feofilov, *Opt. i Spektroskopiya* **13**, 235 (1962) [English transl.: *Opt. Spectry.* **13**, 129 (1962)].

the denominators in the first sum are about 100 times larger than those in the second. (b) The vibronic interaction for the  $4f$  electrons is smaller than that for the  $5d$  electron (i.e.,  $\langle 4f^7 | f_{\mathbf{k}\Gamma^s} | 4f^7 \rangle \ll \langle 4f^6 5d | f_{\mathbf{k}\Gamma^s} | 4f^6 5d \rangle$ ). Evidence for this we find in the appearance of vibronics involving excitation of several phonons in the  $4d$ - $4f$  spectrum, while only first-order vibronic transitions appear in the  $4f$ - $4f$  spectra.

Bron and Wagner<sup>14</sup> have studied the vibronic spectra of divalent RE in alkali halides: Because of the large distortion of the RE-ion vicinity, there exist pseudo-localized vibrations which contribute to the vibronic spectra associated with  $4f$ - $5d$  transitions. These spectra consist of several progressions of sharp lines separated by constant frequency intervals, which are the pseudo-localized vibration frequencies. As can be seen from Fig. 2 and Table V(b) no such behavior is observed for the vibronic transitions of  $\text{Eu}^{2+}$  in  $\text{SrF}_2$ . Also, it was pointed out by Bron and Wagner<sup>14</sup> and shown by Timusk and Buchanan<sup>17</sup> that vibronics associated with  $4f$ - $4f$  transitions were due to nonlocalized vibrations even for cases of large distortion.

We thus conclude that in the present case, the phonons contributing to the vibronic spectra are those of the host crystal. As mentioned above, this is expected to be the case for divalent RE replacing  $\text{Sr}^{2+}$  ions because of their very similar ionic radius and equal valency.

### B. Symmetry of Phonons from Vibronic Transitions

Selection rules for electric dipole vibronic transitions are obtained by considering the symmetry of a given phonon at the RE site. As explained above, this requires reducing the representations of the space group

TABLE V. Vibronic transitions associated with  $5d$ - $4f$  transitions of  $\text{Sm}^{2+}$  and  $\text{Eu}^{2+}$  in  $\text{SrF}_2$ .

(a) $\text{Sm}^{2+}$ , $4f^6 5d(\Gamma_1^-) \rightarrow 7F_1(\Gamma_4^+)$ (at 74°K)			
$\bar{\nu}$ ( $\text{cm}^{-1}$ )	$\Delta\bar{\nu}$	$I_{ab}$	$I_{tot}$
14 804	0	$6 \times 10^{-2}$	$1.3 \times 10^{-1}$
14 792	12		
14 743	61		very weak
14 695	109	$9 \times 10^{-4}$	$8 \times 10^{-3}$
			broad band
14 626	178	$5 \times 10^{-4}$	$9 \times 10^{-2}$
			( $25 \text{ cm}^{-1}$ )
(b) $\text{Eu}^{2+}$ , $4f^6 5d(\Gamma_8^+) \rightarrow 4f^7 8S_{7/2}(\Gamma_6^- + \Gamma_7^- + \Gamma_8^-)$			
24 923.5	0	1	1
24 906.4	17.1	$1.8 \times 10^{-2}$	$1 \times 10^{-1}$
24 860.6	62.9	$3.6 \times 10^{-2}$	$1.4 \times 10^{-1}$
24 792.1	131.4	$4 \times 10^{-2}$	$2.8 \times 10^{-1}$
24 743.0	180.5	$4 \times 10^{-2}$	$2.8 \times 10^{-1}$
24 684.1	239.4	$1.8 \times 10^{-2}$	$2.18 \times 10^{-1}$
24 672.8	250.7	$2.3 \times 10^{-2}$	$2.23 \times 10^{-1}$
24 660.6	262.9	$2.7 \times 10^{-2}$	$2.27 \times 10^{-1}$
24 623.0	300.5	$10^{-1}$	$3.14 \times 10^{-1}$
24 572.7	350.8	$1.3 \times 10^{-1}$	$3.8 \times 10^{-1}$
Many-phonon transitions			
24 503	420	$4 \times 10^{-3}$	$3.27 \times 10^{-1}$
24 449	474	$2.3 \times 10^{-2}$	$3.6 \times 10^{-1}$
24 395	528	$1.8 \times 10^{-2}$	$3.5 \times 10^{-1}$
24 380	543	$1.8 \times 10^{-2}$	$3.6 \times 10^{-1}$
25 274	649	$1.8 \times 10^{-2}$	$3.7 \times 10^{-1}$
24 224	699	$2.3 \times 10^{-2}$	$3.9 \times 10^{-1}$
24 148	775	$9 \times 10^{-3}$	$3.7 \times 10^{-1}$
24 104	819	$5 \times 10^{-3}$	$3.6 \times 10^{-1}$
23 934	989	$4 \times 10^{-3}$	$3.5 \times 10^{-1}$

<sup>17</sup> T. Timusk and M. Buchanan, Phys. Rev. **164**, 345 (1967).

TABLE VI. Space-group reduction coefficients  $O_h^5 \rightarrow O_h$  (phonon branches only).

$O_h$	$\Gamma_1^+$	$\Gamma_2^+$	$\Gamma_3^+$	$\Gamma_4^+$	$\Gamma_5^+$	$\Gamma_1^-$	$\Gamma_2^-$	$\Gamma_3^-$	$\Gamma_4^-$	$\Gamma_5^-$
$O_h^5$										
$X_1^+$	1		1							
$X_6^+$				1	1					
$X_2^-$									1	
$X_3^-$							1	1		
$X_5^-$									1	1
$L_1^+$	1				1					
$L_6^+$			1	1	1					
$L_2^-$							1		1	
$L_3^-$								1	1	1
$W_1$	1		1							1
$W_2$				1			1	1		
$W_3$					1	1		1		
$W_4$		1	1							1
$W_5$				1	1					1
$W_6$										1
$\Delta_1$	1		1							1
$\Delta_4$					1		1	1		
$\Delta_5$				1	1				1	1
$\Delta_1$	1				1		1		1	
$\Delta_3$			1	1	1			1	1	1
$Z_1$	1	1	2							1
$Z_2$				1	1					1
$Z_3$				1	1	1	1	2		1
$Z_4$				1	1					1
$\Sigma_1$	1		1		1					1
$\Sigma_2$		1	1	1						1
$\Sigma_3$				1	1	1		1		1
$\Sigma_4$				1	1		1	1	1	

$O_h^5$  to sums of irreducible representations of  $O_h$ <sup>9,18</sup> (denoted by  $\Gamma_i$ ). Table VI gives the reduction coefficients for space-group representations at some points and directions of high symmetry in the Brillouin zone. Only those representations are given for which there is a phonon branch in  $\text{SrF}_2$ . (A full table is given in Ref. 9.) Using the reduction coefficients, selection rules are calculated as follows. The electronic states involved belong to the irreducible representations  $\Gamma_a$  (initial) and  $\Gamma_b$  (final) of  $O_h$ . In a first-order vibronic transition at low temperatures, a single phonon which transforms like  $\sum_i \Gamma_i$  of  $O_h$  is created. Then, the transition is forbidden if  $\Gamma_a^* \times \Gamma_i \times \Gamma_b$  does not contain  $\Gamma_4^-$  for any  $\Gamma_i$  which appear in the reduction of the phonon space-group representation to site-group representations.

An obvious selection rule is that vibronic transitions between the  $4f^6$  states of  $\text{Sm}^{2+}$  involve phonons which upon reduction  $O_h^5 \rightarrow O_h$  contain odd-parity representations while those between  $4f^{n-1}5d$  and  $4f^n$  of  $\text{Sm}^{2+}$  and  $\text{Eu}^{2+}$  involve even-parity vibrations. A comparison between the phonon energies derived from the frequencies of peaks in the vibronic spectra of  $\text{Eu}^{2+}$  and  $f$ - $d$  transitions of  $\text{Sm}^{2+}$  (Table V) and those of  $f$ - $f$  transitions of  $\text{Sm}^{2+}$  (Tables I-IV) shows that in most cases the phonons are different. The phonons having energy of 131, 250, and 300  $\text{cm}^{-1}$  are the only ones which appear in both cases. However, while the corresponding vi-

<sup>18</sup> R. A. Satten, J. Chem. Phys. **40**, 1200 (1964).

TABLE VII. Electric dipole selection rules for vibronics associated with the transitions  $\Gamma_1^+ \rightarrow \Gamma_i^+$  ( $i=1, \dots, 5$ ).

Phonon	Final electronic state				
	$\Gamma_1^+$	$\Gamma_2^+$	$\Gamma_3^+$	$\Gamma_4^+$	$\Gamma_5^+$
$\Gamma_1^-$				A	
$\Gamma_2^-$					A
$\Gamma_3^-$				A	A
$\Gamma_4^-$	A		A	A	A
$\Gamma_5^-$		A	A	A	A

bronic peaks are strong in the  $\text{Eu}^{2+}$  case, they are extremely weak in the  $f-f$  transitions of  $\text{Sm}^{2+}$ .

Inspection of Table VI shows, however, that except for the points  $\Gamma$ ,  $X$ , and  $L$  of the Brillouin zone, the phonons contain both odd and even parts with respect to the RE site. There are more peaks in the vibronic spectra than can be accounted for by contributions from these points only. Also, the  $\mathbf{k}=0$  Raman active mode ( $\omega_R=280 \text{ cm}^{-1}$ , Ref. 2) does not contribute to the  $\text{Eu}^{2+}$  vibronic spectrum. The  $\mathbf{k}=0$  LO mode ( $\omega_{LO}=392 \text{ cm}^{-1}$  at  $90^\circ\text{K}$ <sup>19</sup>) does not contribute to the  $f-f$  vibronics of  $\text{Sm}^{2+}$  and only the TO mode ( $\omega_{TO}=225 \text{ cm}^{-1}$  at  $90^\circ\text{K}$ <sup>19</sup>) contributes to these spectra (an assignment which is consistent with the Zeeman effect). Thus, the dissimilarity of the  $5d-4f$  vibronics and those within the  $4f$  configuration indicates that the potential set up by the phonons at the RE site has, in most cases, components which are predominantly either even or odd. We can, therefore, classify the phonons which contribute to the  $5d-4f$  vibronics as even-parity vibra-

TABLE VIII. Symmetry of odd-parity phonons at  $\text{Sm}^{2+}$  site ( $O_h$ ).

Phonon energy $\text{cm}^{-1}$	Symmetry from intensities ( $\Gamma_i^-$ )	Symmetry from Zeeman effect ( $\Gamma_i^-$ )
86	3,4,5	
97	2,3,5	3
131	4	
144	4	
157	4	
165	4	
168	2,3,5	3
178	1,3,5	1
183	3,4,5	
194	2,3,4,5	3
202	3,4,5	4
223	2,3,4,5	4
237	4,5	
249	2,3,4,5	4
254	2,3,4,5	4
260	2,3,4,5	4
284	4,5	
294	2,3,4,5	4
300	2,3,4,5	
341	2,3,4,5	

<sup>19</sup> H. W. Verleur and A. S. Barker, Jr., Phys. Rev. **164**, 1169 (1967).

tions and those which contribute to the  $4f-4f$  vibronics as odd-parity vibrations with respect to the RE site.

The effect of additional selection rules due to the cubic symmetry of the RE site is well manifested in the case of the  $4f-4f$  transitions of  $\text{Sm}^{2+}$ . Table VII gives the selection rules for electric dipole vibronic transitions which originate on a  $\Gamma_1^+$  state and terminate at  $\Gamma_i^+$  ( $i=1, \dots, 5$ ). In this study, we determine the symmetry of the phonon at the RE site by examining its contribution to vibronic spectra which involve four distinct final electronic states ( $\Gamma_1^+$ ,  $\Gamma_3^+$ ,  $\Gamma_4^+$ , and  $\Gamma_5^+$ ). From Table VII, we note that the vibronic spectrum associated with the transition  ${}^5D_0(\Gamma_1^+) \rightarrow {}^7F_0(\Gamma_1^+)$  arises from phonons which must have a  $\Gamma_4^-$  component. Although there are several electric multipoles with  $l \leq 5$  which transform like  $\Gamma_4^-$ , the recent work by Timusk and Buchanan<sup>17</sup> shows that for the same transition of  $\text{Sm}^{2+}$  in KBr, the vibronic intensity is mainly due to the electric field produced by the phonons.

TABLE IX. Electric dipole selection rules for vibronics associated with transitions  $\Gamma_1^+ \rightarrow \Gamma_4^+$ ,  $\Gamma_5^+$  with  $\mathbf{H} \parallel [100]$ . Transitions allowed only because of the magnetic field are distinguished by square brackets.

Phonon	Final electronic state						
	$C_{4h}$	$\Gamma_3^+$	$\Gamma_4^+$	$\Gamma_4^+$	$\Gamma_3^+$	$\Gamma_5^+$	$\Gamma_4^+$
$\Gamma_1^-$		$\sigma^+$	$\pi$	$\sigma^-$	$[\sigma^+]$	$\dots$	$[\sigma^-]$
$\Gamma_2^-$		$[\sigma^-]$	$\dots$	$[\sigma^+]$	$\sigma^-$	$\pi$	$\sigma^+$
$\Gamma_3^-$		$\sigma^\pm$	$\pi$	$\sigma^\pm$	$\sigma^\pm$	$\pi$	$\sigma^\pm$
$\Gamma_4^-$		$\pi\sigma^+$	$[\pi]\sigma^\pm$	$\pi\sigma^-$	$\pi\sigma^+$	$\sigma^\pm$	$\pi\sigma^-$
$\Gamma_5^-$		$\pi\sigma^-$	$\sigma^\pm$	$\pi\sigma^+$	$\pi\sigma^-$	$[\pi]\sigma^\pm$	$\pi\sigma^+$

For the transitions  $\Gamma_1^+ \rightarrow \Gamma_3^+$ ,  $\Gamma_4^+$ , and  $\Gamma_5^+$  other multipoles can contribute. By comparing the phonon energies derived from the various vibronic spectra of  $\text{Sm}^{2+}$  and using the selection rules (Table VII) and the reduction coefficients (Table VI), we determine the possible site symmetry of the phonon involved. The results are summarized in Table VIII, second column. In writing down this column, it is borne in mind that certain combinations of  $\Gamma_i^-$  never occur in the reduction  $O_h^5 \rightarrow O_h$ , for points of high symmetry in the Brillouin zone. Thus,  $\Gamma_1^-$  does not appear with  $\Gamma_4^-$  and  $\Gamma_2^-$  does not appear with  $\Gamma_5^-$ . Also it is noted that the vibronic spectrum associated with the transition  $\Gamma_1^+ \rightarrow \Gamma_1^+$  is the strongest of all four examined transitions. It is therefore reasonable to suppose that a phonon which fails to contribute to this spectrum does not contain  $\Gamma_4^-$ . These are the phonons having energies of 97, 168, and  $178 \text{ cm}^{-1}$ . The phonons with energies of 131, 144, 157, and  $165 \text{ cm}^{-1}$  contribute only to the  $\Gamma_1^+ \rightarrow \Gamma_1^+$  spectrum and thus have predominantly a  $\Gamma_4^-$  character. The rest of the observed peaks appear in the  $\Gamma_1^+ \rightarrow \Gamma_1^+$  spectrum

and in at least one more  $\Gamma_1^+ \rightarrow \Gamma_i^+$  spectrum and may consist of several odd components.

### C. Zeeman Effect of $\text{Sm}^{2+}$ Vibronics

A considerable amount of information on the phonons involved in the vibronic transitions is obtained from their Zeeman effect. The relevant electronic transitions are  ${}^5D_0(\Gamma_1^+) \rightarrow {}^7F_1(\Gamma_4^+)$  and  ${}^7F_2(\Gamma_5^+)$ . The application of the magnetic field along the [100] axis reduces  $O_h$  to  $C_{4h}$ . The triply degenerate states split:  $\Gamma_4^+$  (of  $O_h$ )  $\rightarrow$   $\Gamma_1^+$ ,  $\Gamma_3^+$ , and  $\Gamma_4^+$  (of  $C_{4h}$ );  $\Gamma_5^+$  (of  $O_h$ )  $\rightarrow$   $\Gamma_2^+$ ,  $\Gamma_3^+$ , and  $\Gamma_4^+$  (of  $C_{4h}$ ). These irreducible representations are associated with the magnetic quantum number  $m(\text{mod } 4)$  as follows:  $\Gamma_1^+$  with  $m=0$ ,  $\Gamma_2^+$  with  $m=2$ ,  $\Gamma_3^+$  with  $m=-1$ , and  $\Gamma_4^+$  with  $m=+1$ . The phonon states are independent of the magnetic field and thus retain their degeneracy as it is for  $O_h$  symmetry. For high magnetic field (70 kOe), the Zeeman energy is larger than the energy of the ion-phonon interaction.

Under high magnetic field, a vibronic state which arises from a  $|\Gamma_4^+\rangle$  electronic state and  $|\Gamma_i\rangle$  vibrational state will split as follows:

$$|\Gamma_4^+\rangle |\Gamma_i\rangle \xrightarrow{H \parallel [100]} |\Gamma_1^+\rangle |\Gamma_i\rangle + |\Gamma_3^+\rangle |\Gamma_i\rangle + |\Gamma_4^+\rangle |\Gamma_i\rangle.$$

The electric dipole selection rules are derived now, with  ${}^5D_0(\Gamma_1^+)$  being the initial electronic state and all phonons are initially in their ground state. The results are summarized in Table IX. A transition in which  $m_i - m_f = -1$  is governed by the operator  $(x+iy)$  and will appear in  $\sigma^+$  polarization. Now it is noted that certain transitions which are forbidden under  $O_h$  symmetry become allowed with the application of a magnetic field (i.e., for  $C_{4h}$  symmetry). Because the intensity of such transition is proportional to  $(\beta H)^2$  (due to mixing of other electronic states by the magnetic interaction<sup>20</sup>), they are expected to be much weaker than those allowed in  $O_h$  symmetry. In Table IX such cases are denoted by square brackets around the polarization symbol.

The derived selection rules for vibronic Zeeman effect predict definite polarization (either linear or circular) for each phonon species (i.e.,  $\Gamma_i^-$  of  $O_h$ ). However, from Table III it is noted that upon the reduction  $O_h \rightarrow O_h$ , more than one  $\Gamma_i^-$  appears for most phonon branches. In such cases, the degree of polarization of a vibronic Zeeman component might be less. Experimentally, it is observed (Tables II and III) that the vibronic Zeeman components are well polarized. This indicates that only one of the potential components ( $f_{kr}^*$ ) set

up by the phonons at the RE site is contributing to the intensity of the vibronic line. The contribution of other odd-parity components (which transform according to other  $\Gamma_i^-$  of  $O_h$ ) is much smaller and thus undetected. The third column of Table VIII gives the phonon symmetry at the RE site as determined from the vibronic Zeeman effect. In all cases, this  $\Gamma_i^-$  is one of the possible irreducible representations which appear in the second column of Table VIII and which have been determined from intensity consideration. Those phonons for which the symmetry could not be determined from the Zeeman effect are either observed with the  $\Gamma_1^+ \rightarrow \Gamma_1^+$  transition only or give rise to too broad and weak vibronics.

### V. SUMMARY

We have shown that the vibronic transitions associated with  $4f-4f$  and  $4f-5d$  transitions of  $\text{Sm}^{2+}$  and  $\text{Eu}^{2+}$  in  $\text{SrF}_2$  have electric dipole character. The spectra do not have the characteristic appearance of vibronics due to local modes, and they arise from the interaction between the RE ion and the host lattice phonons. The coupling between the ions and the phonons is strongly dependent on the particular electronic states which are involved in the transition. This enables us to determine the parity of the vibrations giving rise to the vibronic spectra and the possible symmetries with respect to the RE site. Out of all potential components set up by a phonon at the RE site, only some contribute significantly to the vibronic intensity. The phonons which contribute to the peaks in the vibronic spectra within the  $4f^6$  configuration are those which set predominantly odd-parity vibrations at the RE site. In the case of vibronic transitions between the  $4f^{n-1}5d$  and  $4f^n$  configurations, phonons with even-parity vibrations are effective. The polarization of the Zeeman components of the  $\text{Sm}^{2+}$  vibronic transitions shows that only one odd-parity vibration contributes to the intensity and that in most cases it is the one which transforms like  $\Gamma_4^-$ . It is reasonable to suppose that this is the contribution of the electric field set up by the phonons.

In this study we were able to determine, to a high precision, the energy and the symmetry at the RE site of those lattice vibrations which contribute to the peaks in the phonon frequency-distribution function. This information is valuable in the analysis of the phonon spectrum of the crystal, when dispersion curves for some directions of high symmetry in the Brillouin zone are available from inelastic neutron scattering.

### ACKNOWLEDGMENTS

The authors wish to acknowledge many helpful discussions with M. D. Sturge. The assistance of W. A. Nordland is much appreciated.

<sup>20</sup> M. H. Crozier, Phys. Rev. Letters **13**, 394 (1964).